J. Fluid Mech. (2006), *vol.* 563, *pp.* 123–132. © 2006 Cambridge University Press
doi:10.1017/S0022112006001509 Printed in the United Kingdom

Kapiza waves as a test for three-dimensional granular flow rheology

By YOËL FORTERRE

IUSTI, Université de Provence, CNRS UMR 6595,
5 rue Enrico Fermi, 13453 Marseille cedex 13, France

(Received 3 April 2006 and in revised form 21 June 2006)

Long-surface-wave instability in dense granular flows down inclined planes is analysed using recently proposed three-dimensional constitutive equations. A full linear stability analysis of the local governing equations is performed and compared to previous experimental results obtained with glass beads. We show that the proposed rheology is able to capture all the features of the instability quantitatively. In particular, it predicts well the behaviour and scaling for the cutoff frequency of the instability observed in the experiments. This result gives strong support for the three-dimensional rheology proposed and suggests new terms in the Saint-Venant equations used to describe free-surface granular flows.

1. Introduction

Finding constitutive equations for dense granular flows has been the subject of many studies in the past decade and is still a matter of debate. For free-surface flows, this absence of local equations has led to the development of depth-averaged models (Saint-Venant equations), which have been applied to various configurations such as flows down inclined planes (Savage & Hutter 1989; Pouliquen & Forterre 2002), free-surface avalanches (Douady, Andreotti & Daerr 1999) and pile collapses (Balmforth & Kerswell 2005; Lajeunesse, Monnier & Homsy 2005). However, although quite successful, these simplified approaches rely on constraining assumptions and lack a general rheological description. The recent local rheology described in GDR MiDi (2004) is in this sense very promising. It consists of writing the rheology as a local friction law, i.e. the local shear stress is proportional to the local normal stress, the friction coefficient being a function of the shear rate and normal stress (da Cruz *et al.* 2005; Iordanoff & Khonsari 2004). Using this scalar rheology, it is possible to describe in a same framework several simple flows varying in one direction, such as plane Couette flows, flows down inclined planes and two-dimensional heap flows (GDR MiDi 2004; Jop, Forterre & Pouliquen 2005). However, this simple scalar law is unable to predict more complex flows, when shears in different directions exist.

A three-dimensional generalization of the local rheology has recently been proposed by Jop, Forterre & Pouliquen (2006). As a first test, these tensorial constitutive equations have been used to quantitatively predict the complex three-dimensional flow pattern obtained when a granular heap flow is confined between rough walls. Another example of granular flow that exhibits shears in different directions is the long-surface-wave instability (or Kapitza instability or roll waves), observed when a granular layer is flowing down a rough inclined plane. When surface waves occur, invariance along the flow is broken and streamwise velocity gradients exist as well as

https://doi.org/10.1017/S0022112006001509 Published online by Cambridge University Press

shears across the layer. This instability should therefore represent another non-trivial configuration for testing the three-dimensional rheology proposed by Jop *et al.* (2006).

In a previous study, Forterre & Pouliquen (2003) had experimentally investigated the linear regime of the long-surface-wave instability using glass beads (flow threshold, dispersion relation). The experimental results were compared with a linear stability analysis of a simple first-order Saint-Venant model incorporating a phenomenological law for the basal friction. Although the agreement was relatively good for the stability threshold, some important features of the instability were not predicted using this simple depth-averaged approach. The most important discrepancy concerned the cutoff frequency of the instability. When the flow was unstable, the Saint-Venant equations predicted that all wavelengths grew, whereas in the experiment a cutoff frequency was observed above which short wavelengths were stabilized. This damping of short wavelengths is likely to come from the dissipation due to flow gradients in the streamwise direction. However, these gradients are not taken into account in a simple first-order model and require knowledge of the full three-dimensional constitutive equations to be computed. A second limitation of the Saint-Venant model used is that it requires an assumption about the shape of the depth velocity profile. For dense flows down inclined planes, discrete numerical simulations suggest that the velocity profile is Bagnold-like (Ertas *et al.* 2001; GDR MiDi 2004). Yet, the Saint-Venant model matched better the experiments when the velocity profile was assumed uniform rather than Bagnold-like (Forterre & Pouliquen 2003). Finally, it is well known in the case of Newtonian fluids that, even when the velocity profile is known, simple first-order Saint-Venant equations fail to predict quantitatively the stability threshold of Kapitza waves. In order to obtain exact results, one has eventually to come back to the full three-dimensional constitutive equations, i.e. the Navier–Stokes equations, and perform a stability analysis from the local mass and momentum equations (Yih 1963).

This is precisely the approach we shall use in this paper. We will take advantage of the recent constitutive equations proposed by Jop *et al.* (2006) to perform a full linear stability analysis of dense granular flows down inclined planes from the local governing equations (§ 2). The results will be compared with the experimental measurements of Forterre & Pouliquen (2003) in order to test the relevance of the proposed rheology (§ 3). In particular, we will focus on the cutoff frequency of the instability and ask whether the proposed rheology is able to predict its experimental scaling. Finally, we will discuss consequences of the proposed tensorial rheology for Saint-Venant models classically used to describe free-surface granular flows (§ 4).

2. Linear stability analysis

In this paper, we use the constitutive equations recently proposed by Jop *et al.* (2006) in order to describe dense granular flows. These equations generalize the scalar rheology presented in GDR MiDi (2004) and Jop *et al.* (2005). The main assumptions consist of neglecting the small variations of volume fraction in dense flows and assuming the pressure to be isotropic. The constitutive equations for the internal stress tensor σ_{ij} are then given by

$$\sigma_{ij} = -P\delta_{ij} + \tau_{ij}, \qquad \tau_{ij} = \frac{\mu(I)P}{\dot{\gamma}}\dot{\gamma}_{ij} \tag{2.1}$$

with

$$\mu(I) = \mu_s + \frac{\mu_2 - \mu_s}{I_0/I + 1}, \qquad I = \dot{\gamma}d/\sqrt{P/\rho_s}, \tag{2.2}$$

https://doi.org/10.1017/S0022112006001509 Published online by Cambridge University Press

where $\dot{\gamma}_{ij} \equiv (\partial_j u_i + \partial_i u_j)$ is the strain rate tensor, $\{u\}_{i=1,2,3}$ are the components of the velocity field and $\dot{\gamma} \equiv \sqrt{\frac{1}{2}\dot{\gamma}_{ij}\dot{\gamma}_{ij}}$. In this rheology, P represents the pressure, d is the particle diameter, ρ_s is the particle density and (μ_s, μ_2, I_0) are constants characterizing the shape of the function $\mu(I)$ (see Jop *et al.* 2006 for a discussion of the law).

Having the constitutive equations, we are now able to write the local governing equations for a granular layer of thickness $h(x,t)$ flowing down an inclined plane that makes an angle θ with respect to horizontal. Considering only two-dimensional perturbations, the local mass and momentum balances for an incompressible flow are

$$\frac{\partial u}{\partial x} + \frac{\partial v}{\partial z} = 0, \tag{2.3}$$

$$\rho_s \phi \left(\frac{\partial u}{\partial t} + u\frac{\partial u}{\partial x} + v\frac{\partial u}{\partial z} \right) = \rho_s \phi g \sin\theta - \frac{\partial P}{\partial x} + \frac{\partial \tau_{xx}}{\partial x} + \frac{\partial \tau_{xz}}{\partial z}, \tag{2.4}$$

$$\rho_s \phi \left(\frac{\partial v}{\partial t} + u\frac{\partial v}{\partial x} + v\frac{\partial v}{\partial z} \right) = -\rho_s \phi g \cos\theta - \frac{\partial P}{\partial z} + \frac{\partial \tau_{zx}}{\partial x} + \frac{\partial \tau_{zz}}{\partial z}, \tag{2.5}$$

where u (resp. v) represents the x (resp. z) velocity component of the flow, ϕ is the constant volume fraction and g is the acceleration due to gravity. The associated boundary conditions are

$$u = v = 0 \quad \text{at} \quad z = 0, \tag{2.6}$$

$$\left.\begin{aligned} \frac{\partial h}{\partial t} + u\frac{\partial h}{\partial x} - v &= 0 \\ -P\frac{\partial h}{\partial x} + \tau_{xx}\frac{\partial h}{\partial x} - \tau_{xz} &= 0 \\ P + \tau_{xz}\frac{\partial h}{\partial x} - \tau_{zz} &= 0 \end{aligned}\right\} \quad \text{at} \quad z = h(x,t). \tag{2.7}$$

Equation (2.6) is the no-slip condition imposed on the rough inclined plane, whereas equations (2.7) mean that the surface $z = h(x,t)$ is a stress-free material interface.

The steady uniform solution of this set of equations, i.e. $h = h_0 = \text{const}$, $u = u_0(z)$, $v = 0$, is easy to obtain (GDR MiDi 2004). The pressure distribution is hydrostatic, $P_0(z) = \rho_s \phi g (h_0 - z)\cos\theta$, and the velocity profile is given by a Bagnold-like expression: $u_0(z) = (2I_\theta/3d)\sqrt{\phi g \cos\theta}({h_0}^{3/2} - (h_0 - z)^{3/2})$ where $I_\theta \equiv \mu^{-1}(\tan\theta)$. In the following, the governing equations and boundary conditions (2.1)–(2.7) will be written in terms of dimensionless variables using the thickness h_0 as the length scale, the depth-averaged velocity $\bar{u}_0 = (1/h_0)\int_0^{h_0} u_0(z)\,\mathrm{d}z = (2/5) I_\theta \sqrt{\phi g d \cos\theta}(h_0/d)^{3/2}$ as the velocity scale and the pressure at the bottom $P_0(0) = \rho_s \phi g h_0 \cos\theta$ as the stress scale. Using this scaling, the two dimensionless control parameters of the problem are the angle θ and the Froude number F defined by

$$F = \frac{\bar{u}_0}{\sqrt{g h_0 \cos\theta}} = \frac{2}{5} I_\theta \sqrt{\phi}\left(\frac{h_0}{d}\right). \tag{2.8}$$

All physical quantities in what follows will be made dimensionless according to the above scalings. However, we will not change the notation for the sake of simplicity.

To study the stability of the steady uniform solution found above, we now perturb the flow about the basic state and seek normal-mode solutions as: $u = u_0(z) + \hat{u}(z)\exp \mathrm{i}(kx - \omega t)$, $v = \hat{v}(z)\exp \mathrm{i}(kx - \omega t)$, $P = P_0(z) + \hat{P}(z)\exp \mathrm{i}(kx - \omega t)$ and $h = 1 + \hat{h}\exp \mathrm{i}(kx - \omega t)$, where k is the longitudinal wavenumber, ω is the pulsation and $(\hat{u}, \hat{v}, \hat{P}, \hat{h}) \ll 1$. By substituting the perturbed flow into the dimensionless version of

https://doi.org/10.1017/S0022112006001509 Published online by Cambridge University Press

equations (2.1)–(2.7) and then linearizing about the basic state, we obtain a set of linear ordinary differential equations for the vertical perturbation $\hat{v}$ and the pressure perturbation $\hat{P}$ given by

$$\left(kF^2\frac{\mathrm{d}u_0}{\mathrm{d}z} - \mathrm{i}k^2\frac{\mathrm{d}g_0}{\mathrm{d}z}\right)\hat{v} + (-kF^2u_0(z) + \mathrm{i}k^2 f_0(z))\frac{\mathrm{d}\hat{v}}{\mathrm{d}z} - \mathrm{i}\frac{\mathrm{d}}{\mathrm{d}z}\left(g_0(z)\frac{\mathrm{d}^2\hat{v}}{\mathrm{d}z^2}\right) + \mathrm{i}k^2\hat{P} - e_0k\frac{\mathrm{d}\hat{P}}{\mathrm{d}z} = -\omega F^2\frac{\mathrm{d}\hat{v}}{\mathrm{d}z}, \quad (2.9)$$

$$(\mathrm{i}kF^2u_0(z) + k^2g_0(z))\hat{v} - 2\frac{\mathrm{d}\eta_0}{\mathrm{d}z}\frac{\mathrm{d}\hat{v}}{\mathrm{d}z} - f_0(z)\frac{\mathrm{d}^2\hat{v}}{\mathrm{d}z^2} - \mathrm{i}ke_0\hat{P} + \frac{\mathrm{d}\hat{P}}{\mathrm{d}z} = \mathrm{i}\omega F^2\hat{v}, \quad (2.10)$$

with the boundary conditions:

$$\hat{v} = \frac{\mathrm{d}\hat{v}}{\mathrm{d}z} = 0 \quad \text{at} \quad z = 0, \quad (2.11)$$

$$\left.\begin{aligned}\hat{v} - \mathrm{i}ku_0(1)\hat{P} &= -\mathrm{i}\omega\hat{P}\\ -\mathrm{i}g_0(1)\frac{\mathrm{d}^2\hat{v}}{\mathrm{d}z^2} + k(\tan\theta - e_0)\hat{P} &= 0\end{aligned}\right\} \quad \text{at} \quad z = 1. \quad (2.12)$$

Here u_0, η_0, e_0, f_0 and g_0 are dimensionless functions of the base state, which are given in Appendix A. Note that we have used the mass conservation equation and the boundary conditions to eliminate the horizontal velocity and free-surface perturbations.

This system of two ordinary differential equations (2.9)–(2.10) together with the four boundary conditions (2.11)–(2.12) forms an eigenvalue problem, i.e. for a given basic flow (u_0, P_0, h_0) and pulsation ω, a non-zero solution ($\hat{v}$, $\hat{P}$) exists only for specific values of the wavenumber k. In order to obtain the full dispersion relation (k,w), we have solved (2.9)–(2.12) numerically using a Chebychev spectral collocation method (Gottlieb, Hussaini, & Orszag 1984). However, as the long-surface-wave instability is a zero-wavenumber instability, it is interesting to perform an asymptotic expansion for small wavenumbers k in order to obtain analytically the stability threshold (Yih 1963). This analysis is presented in Appendix B. The flow is found to be unstable above a critical Froude number F_c given by

$$F_c = \frac{4}{5}\sqrt{1 - \frac{3}{2}\tan^2\theta + \frac{3}{4}\frac{(\mu_2 - \tan\theta)(\tan\theta - \mu_s)}{\mu_2 - \mu_s}\tan\theta}. \quad (2.13)$$

3. Results and comparison with experiments

In this section, predictions of the above stability analysis are compared with the experimental results of Forterre & Pouliquen (2003) using glass beads. To do so, the rheological parameters (μ_s, μ_2, I_0) entering (2.2) must be specified. We have chosen the same values as those used by Jop *et al.* (2005, 2006): $\mu_s = \tan(20.9^\circ)$, $\mu_2 = \tan(32.76^\circ)$ and $I_0 = 0.279$. These values were calibrated using the results on steady uniform flows down rough planes of Forterre & Pouliquen (2003) (see Jop *et al.* 2005 for the computation of these parameters). This choice means that no fitting parameter exists when we compare results from the stability analysis to the experiments.

We first focus on the stability threshold. In figure 1, the critical Froude number F_c predicted by the three-dimensional rheology (equation (2.13), solid line) is presented together with the experimental critical Froude number. A quantitative agreement is observed, although the theoretical threshold is about 10 % higher than the

https://doi.org/10.1017/S0022112006001509 Published online by Cambridge University Press

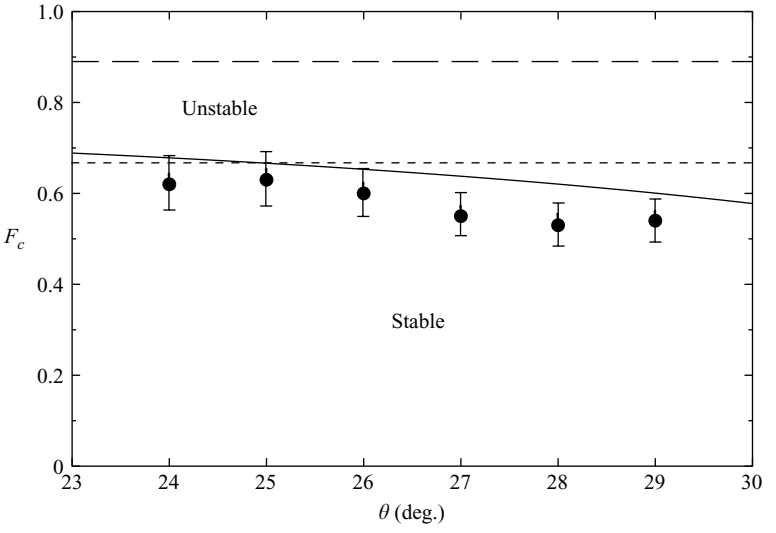


FIGURE 1. Stability diagram of the flow (F_c, θ). Comparison between theory (solid line) and experiments (●, Forterre & Pouliquen 2003). Predictions of the Forterre & Pouliquen (2003) Saint-Venant model are given for comparison: dashed line, Bagnold velocity profile ($\alpha = 5/4$); dotted line, plug flow ($\alpha = 1$).

experimental one. We also present in this figure predictions of the Saint-Venant equations (Forterre & Pouliquen 2003). In this case, there is an adjustable parameter α connected to the shape of the velocity profile across the layer (see Appendix C). As observed with classical fluids, the simple Saint-Venant model strongly overestimates the stability threshold of the Kapitza instability when the shape of the velocity profile is deduced from steady uniform flows, i.e. when the velocity profile is Bagnold-like (dashed line). One obtains a better agreement when the velocity profile is arbitrarily assumed uniform (dotted line).

We now turn to the full dispersion relation of the instability. Experimentally, the dispersion relation was determined by forcing the flow periodically at the entrance and by measuring the spatial growth rate and phase velocity as a function of the forcing frequency. To compare theory and experiment, we therefore solve the eigenvalue problem (2.9)–(2.12) assuming the pulsation ω to be real and the wavenumber k complex. The spatial growth rate is then given by $\sigma = -\mathrm{Im}(k)$ and the phase velocity by $c = \omega/\mathrm{Re}(k)$.

Figure 2 shows a typical dispersion relation obtained numerically together with the experimental results for the same set of parameters: $\theta = 29°$, $F = 1.02$. We observe that the stability analysis using the three-dimensional rheology is able to describe the whole behaviour of the dispersion relation quantitatively. In particular, the theory predicts the existence of a cutoff frequency ω_c for the instability, which is closed to the experimental one (figure 2*a*). This result strongly contrasts with predictions of the Saint-Venant model shown in the same figure (dashed line and dotted line). The first-order Saint-Venant equations do not predict a cutoff frequency for the waves, regardless of the velocity profile's shape. They also strongly underestimate the growth rate when the Bagnold velocity profile is taken into account (dashed line).

Systematic comparison between predictions of the three-dimensional rheology and experiments is presented in figure 3, which gives the experimental and computed cutoff frequency for all Froude numbers and inclinations investigated experimentally. A good agreement is again observed between theory and experiment, although the experimental measurements appear lower than the predictions by 20 %. It is interesting

https://doi.org/10.1017/S0022112006001509 Published online by Cambridge University Press

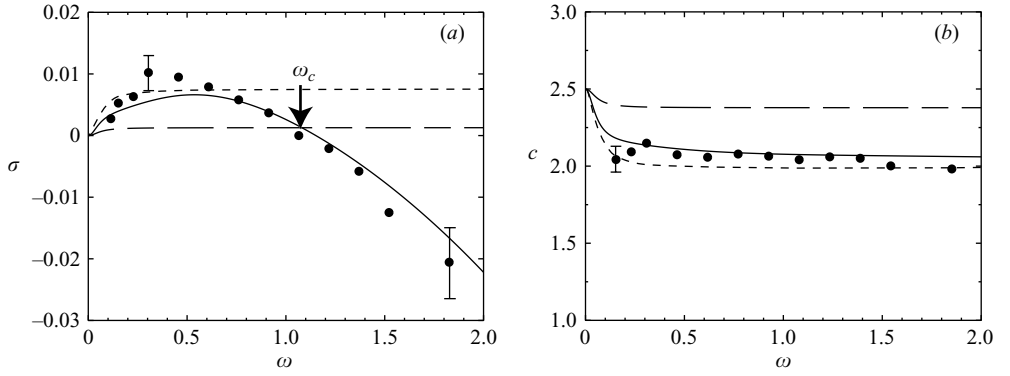


FIGURE 2. Theoretical (solid line) and experimental (●, Forterre & Pouliquen 2003) spatial dispersion relation for $\theta = 29^\circ$ and $F = 1.02$: (*a*) spatial dimensionless growth rate, (*b*) dimensionless phase velocity, as functions of the dimensionless pulsation. Predictions of the Forterre & Pouliquen (2003) Saint-Venant model are given for a Bagnold velocity profile (dashed line, $\alpha = 5/4$) and a plug flow (dotted line, $\alpha = 1$).

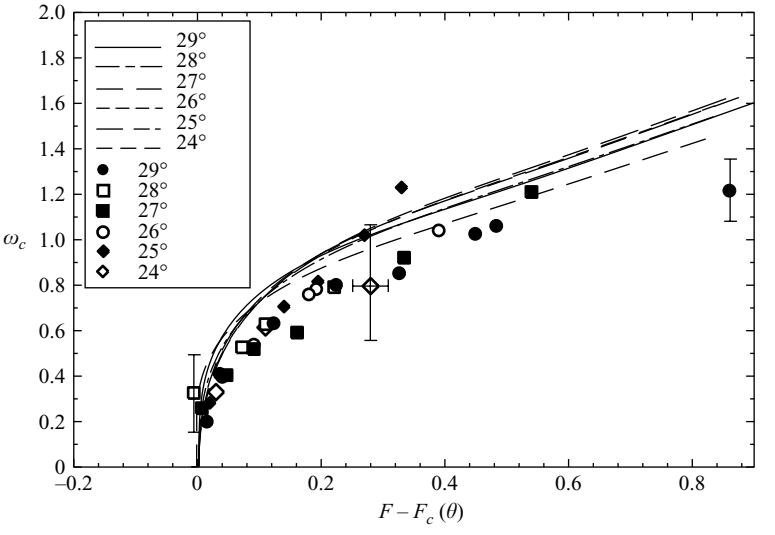


FIGURE 3. Comparison between theory (lines) and experiments (symbols, Forterre & Pouliquen 2003) for the dimensionless cutoff frequency of the instability ω_c above criticality $F - F_c(\theta)$ ($24^\circ \leqslant \theta \leqslant 29^\circ$). The experimental cutoff frequency is made dimensionless using the measured mean velocity and thickness for each point.

to note that both the predicted and experimental neutral stability curves only weakly depend upon the angle of inclination. We will see in the next section that this collapse is not straightforward and strongly reflects the form of the constitutive equations.

4. Discussion

The linear stability analysis of long-wave formation using the constitutive equations proposed by Jop *et al.* (2006) therefore predicts the main features of the instability observed experimentally with glass beads. In particular, the stabilization of short wavelengths, which was not predicted using a simple depth-averaged approach, is now captured quantitatively. This result suggests that the three-dimensional generalization

https://doi.org/10.1017/S0022112006001509 Published online by Cambridge University Press

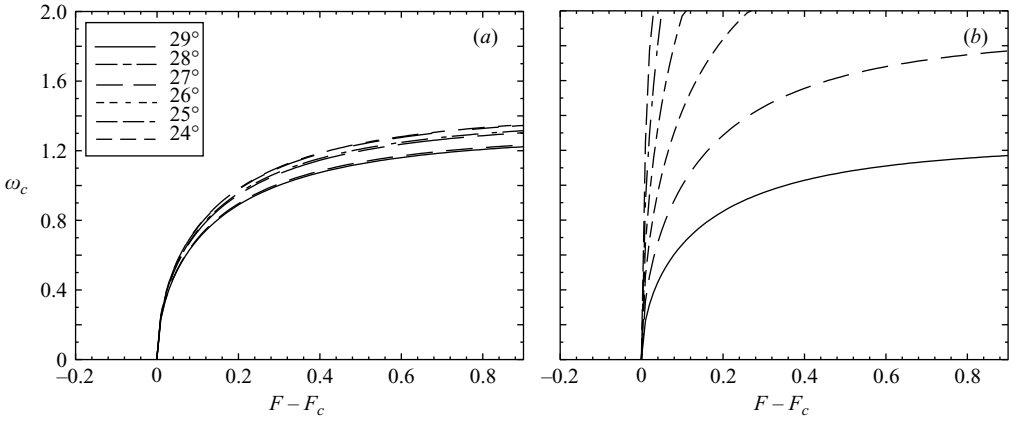


FIGURE 4. (*a*) Neutral stability curves predicted by the modified Saint-Venant model with $a = 0.1$ (see Appendix C). (*b*) Same predictions when the effective viscosity is replaced by a Bagnold-like viscosity $\bar{\eta}_B = a\rho_s d^2 \bar{u}/h$ ($a = 0.2$). In both cases, $\alpha = 1$.

of the local rheology described in GDR Midi (2004) in terms of an 'effective viscosity', $\eta_{\text{eff}} \equiv \mu(I)P/\dot{\gamma}$ (see (2.1)), correctly describes the additional dissipation due to the longitudinal velocity gradients, at least at the onset of wave formation. It is worth noting that no fitting parameter has been used in this study. The constitutive law (2.1)–(2.2) is calibrated using steady flow experiments on inclined planes and is quantitatively the same as the one used by Jop *et al.* (2006) to predict confined heap flows. Moreover, our full stability analysis based on the local governing equations does not introduce extra parameters, as it is usually the case in depth-averaged procedures. The good agreement between the stability analysis and the experiments is therefore additional validation of the three-dimensional law proposed by Jop *et al.* (2006).

Knowledge of the local three-dimensional rheology also allows us to modify the Saint-Venant equations used to describe free-surface granular flows, in order to capture the longitudinal dissipation. Formally, this requires an expansion of the shallow-water approximation up to the second order. Here we instead adopt a heuristic approach by simply adding to the Saint-Venant model used by Forterre & Pouliquen (2003) the depth-averaged longitudinal viscous stress: $\partial(\int_0^h \tau_{xx}\,\mathrm{d}z)/\partial x$. Using the constitutive law (2.1)–(2.2) and rewritting the effective viscosity as $\eta_{\text{eff}} = \rho_s d^2(\mu(I)/I^2)\dot{\gamma}$, we can approximate this term as

$$\frac{\partial}{\partial x}\int_0^h \tau_{xx}\,\mathrm{d}z = \frac{\partial}{\partial x}\int_0^h 2\rho_s d^2 \frac{\mu(I)}{I^2}\dot{\gamma}\frac{\partial u}{\partial x}\,\mathrm{d}z \approx \frac{\partial}{\partial x}\left(\bar{\eta}_{\text{eff}}\frac{\partial h\bar{u}}{\partial x}\right), \tag{4.1}$$

where $\bar{\eta}_{\text{eff}} \sim \rho_s d^2(\tan\theta/I_\theta^2)\bar{u}/h$ is a mean effective viscosity and $\bar{u} = (1/h)\int_0^h u\,\mathrm{d}z$ is the depth-averaged velocity (here and hereafter, the quantities are not dimensionless for clarity). The resulting modified Saint-Venant model is given in Appendix C. A linear stability analysis of these equations leads to results shown in figure 4(*a*) (computation not shown). The cutoff frequency of the instability is now predicted, as well as the collapse of the neutral stability curves for different angles of inclination. It is interesting to investigate to what extent this collapse is constrained by the special form of the effective viscosity embedded in the three-dimensional rheology. To do so, we present in figure 4(*b*) the prediction of the same model, but with the mean effective viscosity $\bar{\eta}_{\text{eff}}$ replaced by a simple Bagnold scaling $\bar{\eta}_B \sim \rho_s d^2 \bar{u}/h$. The striking result is that the neutral curves now clearly split into the range of angles explored experimentally. A closer

https://doi.org/10.1017/S0022112006001509 Published online by Cambridge University Press

investigation of the longitudinal stress (4.1) reveals that this difference comes from the particular behaviour of the effective viscosity close to the flow threshold: $\bar{\eta}_{\rm eff}$ diverges when $I_\theta \to 0$ whereas $\bar{\eta}_B$ vanishes at threshold. The collapse of the cutoff frequencies is therefore a non-trivial signature of the underlying three-dimensional rheology and gives more support for the relevance of the law proposed by Jop *et al.* (2006).

5. Conclusion

In this paper, we have performed a full linear stability analysis of granular flows down inclined planes using the three-dimensional constitutive equations recently proposed by Jop *et al.* (2006). We have shown that, without any fitting parameters, the predictions of the stability analysis are in quantitative agreement with the experiment of Forterre & Pouliquen (2003) using glass beads. In particular, the theory quantitatively predicts the behaviour of the cutoff frequency of the instability, not captured by previous depth-averaged approaches.

Our study provides a new validation of the three-dimensional law proposed by Jop *et al.* (2006), in a case where velocity gradients perpendicular to the main shear play an important role. Other geometries involve a complex three-dimensional flow pattern, such as rotating drum flows or pile collapses. It would be interesting to test the three-dimensional rheology on these well-documented examples, in order to better explore the validity of the law. Limits of this rheology exist, which have been described in Jop *et al.* (2006). They mainly concern the transition between the solid and liquid-like behaviour of granular matter close to the flow threshold, where non-local effects and hysteretic phenomena occur. The proposed rheology also does not predict the small variations of volume fraction observed in dense flows (see however Pouliquen *et al.* 2006 for a simple attempt to capture the volume fraction). Another important issue concerns the extension of this approach to flows composed of more complex particles like sand, for which the instability properties are peculiar (Forterre & Pouliquen 2003). It has already been shown that the simple local rheology $\mu(I)$ is unable to describe the flow of sand down inclined planes (GDR MiDi 2004). Our stability analysis therefore cannot be applied to predict quantitatively the instability properties in this case. However, despite these limits, the proposed rheology provides a minimal model that could be used to quantitatively predict the main 'viscous' properties of granular flows, when a full tensorial relation is needed. The three-dimensional rheology could also help to improve the Saint-Venant models used to describe free-surface granular flows. In this study, we have proposed a simple approach that contains the longitudinal 'viscous' dissipation. More precise depth-averaged models, in the spirit of those written for Newtonian (Ruyer-Quil & Manneville 2000) or visco-plastic fluids (Balmforth & Liu 2004), still have to be derived.

I would like to thank Pierre Jop and Olivier Pouliquen for stimulating discussions.

Appendix A

The dimensionless functions of the base state given in (2.9)–(2.12) are

$$\left.\begin{aligned} &u_0(z) = (5/3)\left(1-(1-z)^{3/2}\right),\ \eta_0(z) = (2/5)\tan\theta\,(1-z)^{1/2},\\ &e_0 = \tan\theta - [(\mu_2 - \tan\theta)(\tan\theta - \mu_s)/(2(\mu_2 - \mu_s))],\\ &f_0(z) = \eta_0(z) - [(4/25)\,(\tan\theta - 2e_0))\,(\mathrm{d}u_0/\mathrm{d}z)],\\ &g_0(z) = \eta_0(z) + [(4/25)\,(\tan\theta - 2e_0))\,(\mathrm{d}u_0/\mathrm{d}z)]. \end{aligned}\right\} \qquad \text{(A 1)}$$

https://doi.org/10.1017/S0022112006001509 Published online by Cambridge University Press

Note that the functions $f_0(z)$ and $g_0(z)$ vanish at the free surface $z=1$. This introduces a difficulty when solving the eigenvalue problem (2.9)–(2.12) since the product $g_0(z)\,\mathrm{d}^2\hat{v}/\mathrm{d}z^2$ appears in the boundary condition at $z=1$. To remove this singularity, we eliminate $\mathrm{d}^2\hat{v}/\mathrm{d}z^2$ in (2.9)–(2.12) by introducing the new variable $\hat{A}(z) \equiv g_0(z)\mathrm{d}^2\hat{v}/\mathrm{d}z^2$, which is regular when $z \to 1$.

Appendix B

Here we give the asymptotic expansion $k \to 0$ of the eigenvalue problem (2.9)–(2.12) in the case of temporal stability, i.e. k is real and ω is complex. We follow the procedure proposed originally by Yih (1963) in the context of Newtonian fluids and introduce the stream function $\hat{\psi}(z)$ and the phase velocity $c(k)$ defined by $\hat{\psi} \equiv (\mathrm{i}/k)\hat{v}$ and $c \equiv \omega/k$. The stream function $\hat{\psi}$, the pressure $\hat{P}$ and the phase velocity c are then expanded in powers of the small parameter k as

$$\left.\begin{aligned} \hat{\psi} &= \hat{\psi}^{(0)} + \mathrm{i}k\hat{\psi}^{(1)} + k^2\hat{\psi}^{(2)} + \cdots, \\ \hat{P} &= \hat{P}^{(0)} + \mathrm{i}k\hat{P}^{(1)} + k^2\hat{P}^{(2)} + \cdots, \\ c &= c^{(0)} + \mathrm{i}kc^{(1)} + k^2c^{(2)} + \cdots. \end{aligned}\right\} \tag{B 1}$$

The solution of (2.9)–(2.12) at order zero gives

$$\left.\begin{aligned} &\hat{\psi}^{(0)}(z) = (1-z)^{3/2} + (3/2)z - 1, \\ &\hat{P}^{(0)}(z) = 3/5, \\ &c^{(0)} = 5/2. \end{aligned}\right\} \tag{B 2}$$

Note that the eigenfunctions $\hat{\psi}$ and the pressure $\hat{P}$ are arbitrarily normalized in order to have $\hat{\psi}(1) = 1/2$. To find the stability threshold, the problem has to be solved at order one, which after some algebra gives

$$\left.\begin{aligned} \hat{\psi}^{(1)}(z) &= (2(\tan\theta - e_0))^{-1}\big[-(5/48)F^2(1-z)^4 + \zeta(1-z)^{5/2} \\ &\qquad + (3/2)e_0\tan\theta\, z^2 + 5\zeta(1-z)^{3/2} + \gamma z + \delta\big], \\ \hat{P}^{(1)}(z) &= -(3/5)\tan\theta(1-z) - (3/2)(1-z)^{1/2} + \hat{P}^{(1)}(1), \\ c^{(1)} &= (2(\tan\theta - e_0))^{-1}[(25/16)F^2 - 1 + (3/2)e_0\tan\theta], \end{aligned}\right\} \tag{B 3}$$

with $\zeta = (5/6)F^2 - (2/5)(1 + e_0\tan\theta)$, $\gamma = -(5/12)F^2 - 5\zeta$, $\delta = (15/16)F^2 + 4\zeta$ and $\hat{P}^{(1)}(1) = (6/5)[\hat{\psi}^{(1)}(1) - c^{(1)}\hat{P}^{(0)}(1)]$. The flow is unstable when $c^{(1)} > 0$.

Appendix C

The modified Saint-Venant model is given by

$$\frac{\partial h}{\partial t} + \frac{\partial h\bar{u}}{\partial x} = 0, \tag{C 1}$$

$$\rho_s\phi\left(\frac{\partial h\bar{u}}{\partial t} + \alpha\frac{\partial h\bar{u}^2}{\partial x}\right) = \left(\tan\theta - \mu_b(\bar{u}, h) - \frac{\partial h}{\partial x}\right)\rho_s\phi g h\cos\theta + a\rho_s d^2\frac{\tan\theta}{I_\theta^2}\frac{\partial}{\partial x}\left(\frac{\bar{u}}{h}\frac{\partial h\bar{u}}{\partial x}\right). \tag{C 2}$$

Equation (C 1) is the depth-averaged mass conservation. Equation (C 2) is the depth-averaged momentum equation along the x-direction. The last term of (C 2) is

https://doi.org/10.1017/S0022112006001509 Published online by Cambridge University Press

new and responsible for the damping of the short wavelengths (a is an unknown dimensionless coefficient coming from (4.1)). The coefficient α is related to the assumed velocity profile across the layer and $\mu_b(\bar{u}, h)$ is the bottom friction given by $\mu_b(\bar{u}, h) = \mu_s + ((\mu_2 - \mu_s)/((\beta h\sqrt{gh}/\bar{u}L_0) + 1))$, where $\beta/L_0 = 0.295 I_0/d$ (see Jop *et al.* 2005 for the connection between $\mu_b(\bar{u}, h)$ and $\mu(I)$).

REFERENCES

Balmforth, N. J. & Kerswell, R. R. 2005 Granular collapse in two dimensions. *J. Fluid Mech.* **538**, 399–428.

Balmforth, N. J. & Liu, J. J. 2004 Roll waves in mud. *J. Fluid Mech.* **519**, 33–54.

da Cruz, F., Eman, S., Prochnow, M., Roux, J.-N. & Chevoir, F. 2005 Rheophysics of dense granular materials: Discrete simulation of plane shear flows. *Phys. Rev.* E **72**, 021309.

Douady, S., Andreotti, B. & Daerr, A. 1999 On granular surface flow equations. *Eur. Phys. J.* B **11**, 131–142.

Ertas, D., Grest, G. S., Halsey, T. C., Levine, D. & Silbert, E. 2001 Gravity-driven dense granular flows. *Europhys. Lett.* **56**, 214–220.

Forterre, Y. & Pouliquen, O. 2003 Long-surface-wave instability in dense granular flows. *J. Fluid Mech.* **486**, 21–50.

GDR MIDI 2004 On dense granular flows. *Eur. Phys. J.* E **14**, 341–365.

Gottlieb, D., Hussaini, M. Y. & Orszag, S. A. 1984 Theory and application of spectral methods. In *Spectral Methods for Partial Differential Equations* (ed. R. G. Voight, D. Gottlieb & M. Y. Hussaini). SIAM.

Iordanoff, I. & Khonsari, M. M. 2004 Granular lubrication: toward an understanding betweeen kinetic and fluid regime. *ASME J. Tribol.* **126**, 137–145.

Jop, P., Forterre, Y. & Pouliquen, O. 2005 Crucial role of side walls for granular surface flows: consequence for the rheology. *J. Fluid Mech.* **541**, 167–192.

Jop, P., Forterre, Y. & Pouliquen, O. 2006 A constitutive law for dense granular flows. *Nature* **441**, 727–730.

Lajeunesse, E., Monnier, J. B. & Homsy, G. M. 2005 Granular slumping on a horizontal surface. *Phys. Fluids* **17**, 103302.

Pouliquen, O., Cassar, C., Jop, P., Forterre, Y. & Nicolas, M. 2006 Flow of dense granular material: towards simple constitutive laws. *J. Statist. Mech.* (to appear).

Pouliquen, O. & Forterre, Y. 2002 Friction law for dense granular flows: application to the motion of a mass down a rough inclined plane. *J. Fluid Mech.* **453**, 133–151.

Ruyer-Quil, C. & Manneville, P. 2000 Improved modeling of flows down inclined planes. *Eur. Phys. J.* B **15**, 357–369.

Savage, S. B. & Hutter, K. 1989 The motion of a finite mass of granular material down a rough incline. *J. Fluid Mech.* **199**, 177–215.

Yih, C. S. 1963 Stability of liquid flow down an inclined plane. *Phys. Fluids* **6**, 321–330.

https://doi.org/10.1017/S0022112006001509 Published online by Cambridge University Press